The International Journal of Cardiovascular Imaging (2019) 35:1691–1699
https://doi.org/10.1007/s10554-019-01610-z

ORIGINAL PAPER

Comprehensive cardiac phenotyping in large animals: comparison of pressure–volume analysis and cardiac magnetic resonance imaging in pig post-myocardial infarction systolic heart failure

Philip W. J. Raake[1,4] · Jens Barthelmes[1] · Birgit Krautz[1] · Sebastian Buss[1] · Regina Huditz[1] · Philipp Schlegel[1] · Christophe Weber[1] · Manfred Stangassinger[3] · Uwe Haberkorn[2] · Hugo A. Katus[1] · Patrick Most[1] · Sven T. Pleger[1]

Received: 3 April 2018 / Accepted: 28 June 2018 / Published online: 5 May 2019

Abstract
Large animal ischemic cardiomyopathy models are widely used for preclinical testing of promising novel therapeutic approaches. Pressure volume (PV) loop analysis and cardiac magnetic resonance imaging (CMRI) allow functional and morphological phenotyping. In this study we performed a comparative analysis of both methods highlighting the strength of each and their synergistic potential. Myocardial infarction (MI) was created in German farm pigs (German Landrace) by 2 h LCX occlusion (n = 11) and subsequent reperfusion. Cardiac function was assessed by PV-loops and CMRI 56 and 112 days post-MI. Two hours occlusion of the LCX led to mid-size left ventricular (LV) MI represented by high-sensitive troponin T (hsTnT) 3 days post-MI, correlating well with cardiac CMRI late enhancement. CMRI determined end-diastolic and end-systolic volumes significantly increased post-MI, while ejection fraction was reduced in infarcted animals compared to the sham group (n = 6). PV-loop derived preload-insensitive parameters of systolic and diastolic function were diminished post-MI compared to sham animals while preload-dependent parameters only deteriorated in advanced HF. PV-loop analysis significantly correlates with CMRI analysis of cardiac function in pig post-MI ischemic cardiomyopathy. PV-Loop analysis accurately quantifies LV volumetry and function in post-MI HF, and thus eccentric LV morphology. PV-loop analysis correlates well to cardiac MRI. Preload–insensitive parameters show high sensitivity to quantify HF while preload–sensitive parameters are not able to quantify early-stages of LV HF.

Keywords Heart failure · Ischemic cardiomyopathy · Pig model · Cardiac function · Pressure–volume loops · Cardiac magnetic resonance imaging

Introduction

Ischemic cardiomyopathy remains a leading cause of mortality in western countries [1, 2]. Evolving novel therapies, recently successful in small animal models, demand preclinical testing in larger animal models ahead of clinical trials [3–9]. A widely established preclinical model is the pig model of post myocardial infarction (MI) ischemic cardiomyopathy [5]. This model is typically created by temporal occlusion of the left anterior descending (LAD) or left circumflex (LCX) coronary artery [8, 9]. Infarct-size can be defined by the exact position of LAD or LCX temporary ligation. Induction of large MI in this model causes excess of acute mortality. Therefore, often small to mid-size MI is created sometimes impeding the proof of developed systolic left ventricular (LV) heart failure (HF). What is more, therapeutic effects of novel treatment strategies aiming to target

✉ Philip W. J. Raake
philip.raake@med.uni-heidelberg.de

1 Department of Internal Medicine III, Cardiology, University of Heidelberg, Heidelberg, Germany

2 Department of Nuclear Medicine, University of Heidelberg, Heidelberg, Germany

3 Institute for Animal Physiology, Ludwig-Maximilians-University Munich, Munich, Germany

4 Department of Internal Medicine III, University Hospital Heidelberg, University of Heidelberg, Im Neuenheimer Feld 410, 69120 Heidelberg, Germany

morphological aspects such as infarct size and/or functional aspects such as LV systolic and diastolic function need to be precisely detected and quantified. Therefore, it is important to establish most sensitive tools for functional and morphological assessment of the LV in HF.

LV function and infarct size is often determined by echocardiography and/or LV pressure assessment, which cannot exactly quantitate loss of myocardium, infarct-size as well as subtle changes in LV function.

In the present study we compared the "gold standard" cardiac magnetic resonance imaging (MRI) to admittance-derived pressure–volume (PV) loops for detailed and exact quantitative assessment of LV function and morphology in a model of pig systolic HF caused by mid-sized MI. Both methods can deliver volumetry of the LV as well as LV function in HF. Although these techniques are widely used, limited comparative data in a large animal model of systolic HF is available [10, 11]. In the current study, we aimed to examine the most sensitive technique with regard to LV function and LV morphology as well as synergistic aspects.

Materials and methods

Animal model

The present investigation was carried out according to the 'Guide for the Care and Use of Laboratory Animals' and was approved by the Animal Care and Use Committee. German Landrace pigs (male [caponized] and female) were randomly (age-and sex-matched) assigned to sham operation or MI.

Model of myocardial infarction and study protocol

Pigs (German Landrace; n = 11 myocardial infarction, n = 6 sham) were anaesthetized and monitored as described previously [8, 9]. LV myocardial infarction was created as previously described [8, 9]. The right carotid artery was dissected free and a catheter introducer sheath was placed. Via this sheath a 7F guiding catheter (7F Judkins right, Cordis, Johnson and Johnson, Waterloo, Belgium) was advanced into the ostium of the left coronary artery and a 0.014" standard guiding (Balance Middle Weight, Abbott, Santa Clara, CA, USA) wire placed in the distal portion of the LCX and a percutaneous transluminal coronary angioplasty (PTCA) balloon (Emerge 3.0 × 12 mm, Boston Scientific, Natick, MA, USA) was placed at the ostium of the LCX and inflated at 14 atm [8, 9]. Coronary angiography allowed for confirmation of proximal LCX occlusion by the PTCA balloon. After 2 h of LCX occlusion the PTCA balloon was deflated and all catheters and introducer sheaths were removed. Sham operation was carried out in a similar fashion except LCX balloon occlusion.

Three days after MI, peripheral venous blood was sampled to determine high-sensitive cardiac troponin T (hsTnT) by quantitative electrochemiluminescense immunoassay (Roche Diagnostics, Mannheim, Germany) [12]. Fifty-six days (8 weeks) later animals were anesthetized again and cardiac function was determined by admittance-derived PV-loops and cardiac MRI accompanied by blood sample collection. To allow for longer term follow-up animals were anesthetized 112 days (16 weeks) post-MI and cardiac function was determined by admittance-derived PV-loops and cardiac MRI; in addition a blood sample was collected for biomarker assessment. Animals were euthanized for standardized autopsy. Tissue samples were collected for molecular analyses.

Cardiac magnetic resonance imaging (MRI)

Cardiac function was analyzed by cardiac MRI at day 56 and day 112 in a clinical 1.5-T whole-body scanner (Achiva, Philips, Best, Netherlands).

To assess left ventricular function a vector-ECG-gated regular SSFP sequence (temporal resolution of 28 ms at a heart rate of 60 beats per minute) was performed to obtain cine images of the three long- axis and 16–18 short-axis views, 8 mm in thickness with no interslice gap covering the whole left ventricle from base to apex (echo time [TE] 1.4 ms; repetition time [TR] 2.8 ms; flip angle 60°; spatial resolution $2.4 \times 2.5 \times 8$ mm^3; 40 phases per cardiac cycle). A gadolinium- based contrast medium (Magnevist, Bayer Vital, Germany; 0.2 mmol/kg) was then administered intravenously. Ten minutes later, contrast-enhanced images were acquired in the same orientation as the cine images using a segmented inversion-recovery gradient-echo pulse sequence triggered to end-diastole. The inversion time was adapted individually to suppress signal of normal myocardial tissue (echo time [TE] 1.1 ms; repetition time [TR] 3.0 ms; flip angle 15°; spatial resolution 1.5×1.7 mm^2).

A conventional Philips work station (ViewForum, Philips Medical Systems, Best, Netherlands) was used to determine all cardiac MRI data like end- systolic, end- diastolic volume [ml] and LV ejection fraction [%] by manually defining the endocardial and epicardial border in all collected short-axis views.

Admittance-derived left ventricular pressure–volume-loop analysis

Immediately after the MRI was performed at day 56 and day 112, the animals were brought back to the operation room facilities to assess stroke volume by transthoracic Doppler echocardiography (Sonos 7500, Philips, Hamburg, Germany). Next, pressure Volume loops were recorded under steady-state conditions. The inferior vena cava (IVC) was

then briefly occluded in order to achieve temporary preload reduction [13]. Two 9F catheter sheaths were placed in either carotid artery. A single segment tetrapolar pressure volume (PV)-catheter (7F Pressure Volume Catheter Pig Tail no Lumen FTH-7018B-E248B, Scisense systems, London, ON, CA) was placed in the LV to record PV-loops by the Scisense ADVantage 997B admittance based system and iWorx 228 on a personal computer running LabScribe 2 (iWorx, Dover, NH, USA). The integrated pressure probe was calibrated against atmosphere as recommended immediately before and after advancement of the catheter in the LV. In case of disparate values before and after measurement, the latter was used for pressure calibration. An electrocardiogram was recorded to determine end-systole and end-diastole. Stroke volume and a general estimate of the ratio of myocardial conductivity to permittivity of 1,000,000 S/F for sham operated animals and 1,200,000 S/F were set in the recording hardware. During real-time recording of pressure volume loops a balloon catheter (26 × 50 mm Medtronic CV-26, Medtronic, Minneapolis, MN, USA) was advanced in the IVC using fluoroscopy. Steady state was checked before the ventilator was disconnected for ca. 40 s. Consequently the balloon was briefly inflated (for a median duration of 12 heart beats corresponding to ca. 9 s. on average) to record occlusion loops over a pressure range of 18.8 ± 2.0 mmHg.

Contractility was assessed by two load-insensitive parameters derived from IVC occlusion loops, the end-systolic pressure volume relation (ESPVR) and preload recruitable stroke work (PRSW). ESPVR was modeled as curvilinear as suggested by Burkhoff using the equation: $P_{es} = a \cdot V_{es}^2 + b \cdot V_{es} + c$, where P_{es} and V_{es} are pressure and respective volume at end-systole [14]. The constants a, b, and c are derived by polynomial regression. The discriminant of this equation serves as an index of the end-systolic elastance Ees, so that $E_{es} := \sqrt{b^2 \cdot 4ac}$. PRSW was assessed by the linear regression of stroke work with the end diastolic volume [14].

Diastolic properties were assessed by the end-diastolic pressure volume relation (EDPVR), which is intrinsically non-linear. As suggested previously we report the chamber stiffness constant β (dP/dV) resulting from curve fit to $P_{ed} = C^{\beta V}$, where P_{ed} is end-diastolic pressure, V the corresponding end-diastolic Volume, and C a constant base resulting from the curve fit [14].

Statistical analysis

Data in tables are generally expressed as mean ± one standard error of the mean (SEM). Data Analysis was performed using LabScribe 2 (iWorx, Dover, NH, USA), JMP9 (SAS, Cary, NC, USA), and SPSS 20 (IBM, Armonk, NY, USA).

Homoskedasticity was tested by Levène's test and residual plots, normal distribution was assessed visually by Q–Q plots due to small sample size. An unpaired two-tailed Student's or Welch's *t* test was performed accordingly. Computed p-values are reported and $p < 0.05$ is considered significant.

ESPVR discriminant (Ees) and intercept with volume axis as well as PRSW slope and intercept with volume axis are each compared group-wise by an ANOVA as omnibus test and, if a significant difference is detected, Fisher's Least Significant Difference procedure is used as post hoc test.

Mean-difference plots were created for comparison of admittance-derived pressure volume loops and cardiac magnetic resonance imaging as suggested by Bland and Altman [15]. Pearson's product moment coefficient R^2 is reported for ordinary linear regressions if it is highly unlikely to be zero ($p < 0.001$).

Results

Induction of myocardial infarction caused by temporary LCX ligation - hsTNT at day 3 post-MI correlates to infarct size

Two hours temporary LCX occlusion resulted in a significant rise in serum high sensitive Troponin T (hsTnT) levels at day three post-MI indicating significant loss of viable myocardium (Fig. 1a, b) as compared to sham (hsTnT MI 1542 ± 274 pg/mL vs. sham ≤ 3 ± 0 pg/mL, $p < 0.05$). We analyzed infarct size 56 and 112 days post-MI by assessment of gadolinium late enhancement (LE) of the LV mass by cardiac MRI. Pigs showed small to mid-size post-MI scar formation of the LV as compared to sham animals (LE on day 56; 14.49% ± 1.89% vs. LE on day 112; 14.14% ± 1.91%). Importantly, assessment of the serum marker hsTnT (obtained 3 days post-MI) and measurement of left ventricular LE by cardiac MRI showed significant correlation on day 56 and day 112 (Fig. 1a, b).

Cardiac magnetic resonance imaging (MRI) shows mild-to moderate LV heart failure after temporary LCX occlusion

To assess LV function and LV remodeling cardiac MRI is considered to be the "gold standard". Thus, LV function and LV volumes were analyzed by cardiac MRI on day 56 and day 112 post-MI. Compared to the sham group, post-MI pigs showed significant end-diastolic and end-systolic enlargement of the LV both at day 56 and at day 112 (Fig. 2a, b). In addition, LV ejection fraction was significantly reduced in post-MI pigs as compared to sham animals at day 56 as well as at day 112, although deterioration of the LV systolic function was mild to moderate (Fig. 2c).

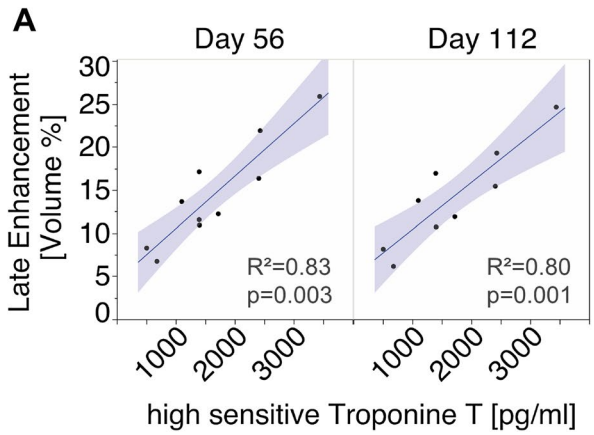

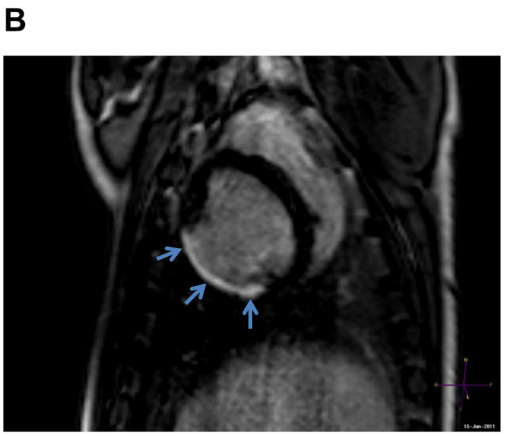

Fig. 1 Pig model of ischemic cardiomyopathy. Following two hours of LCX balloon occlusion a rise in cardiac high sensitive troponine T (hsTnT) was observed 3 days post-MI, which correlates to LV area of cardiac MRI Gadolinium late enhancement 56 and 112 days post-MI (**a**). Representative image of cardiac MRI Gadolinium late-enhancement demarking the LV area of MI (**b**, light blue arrows)

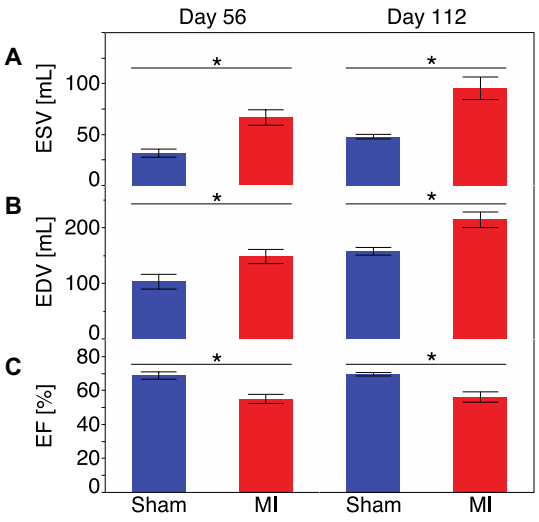

Fig. 2 Cardiac MRI shows significant enlargement of the LV and reduction of LV cardiac function 56 and 112 days post-MI. *ESV* endsystolic volume, *EDV* enddiastolic volume, *EF* ejection fraction. Mean ± SEM, *p < 0.05

Admittance-derived pressure–volume relations show enlargement of LV dimensions and LV heart failure

Measurements were taken at baseline and under brief occlusion of the inferior vena cava (IVC) for preload reduction. Representative average steady state PV-loops with IVC occlusions show typical loop morphological changes for the two groups. Post-MI pigs showed increased ESV and EDV corresponding to a rightward shift of the loop. Furthermore, a discretely lower ESP (Table 1) with lower pulse amplitudes contributes to the aspect of moderate rounding of the PV-loops (Fig. 3).

Preload-sensitive parameters of systolic LV function (+dP/dt) and diastolic LV function (-dP/dt, Tau) were not significantly altered at day 56. However, proceeding of HF caused that preload-sensitive parameters were significantly reduced in post-MI pigs at days 112 as compared to the sham group (Figs. 4d, e, 5a, b and Table 1).

Preload-independent parameters of systolic (end-systolic pressure volume relationship, preload recruitable stroke work) and diastolic (end-diastolic pressure volume relationship) function were significantly reduced both at day 56 and at day 112 post-MI (Figs. 4a–c, 5c and Table 1). Thus, only preload-independent parameters show—early—significant deterioration of the LV in mild to moderate systolic HF at day 56.

Comparison of PV-loops and cardiac MRI demonstrates correlation of LV volumes and LV function while only preload-independent parameters show adequate sensitivity in early stages of moderate HF

The ordinary linear regression of volumes derived by either method shows highly significant ($p < 0.001$) correlations of $R^2 = 0.95$ for ESV, $R^2 = 0.98$ for EDV, and $R^2 = 0.91$ for the derived EF (Fig. 6a–c). Mean vs. difference plots (Bland–Altman-plots) show no significant measurement bias with 95% confidence intervals of the three mean biases all including zero (Fig. 6a–c). In moderate systolic HF only preload-independent parameters show sufficient sensitivity to detect deterioration of LV function in early-stages of HF 56 days post-MI. Infarct size (in % of LV) as determined by cardiac MRI area of late Gadolinium enhancement is significantly and inversely correlated to EF determined by admittance-derived PV-loops at both 56 ($R^2 = 0.51$, $P < 0.05$) and 112 ($R^2 = 0.51$, $P < 0.05$) days (Fig. 7).

Table 1 Summary of all collected physiological, PV-loop and cardiac MRI data

	2 months					4 months				
	Sham		MI		t-test	Sham		MI		t-test
	Mean	± SEM	Mean	± SEM	p-value	Mean	± SEM	Mean	± SEM	p-value
Body weight (kg)	43.0	4.6	50.8	4.7	0.280	88.7	3.1	87.9	4.5	0.889
Number of loops analyzed	30.4	1.6	30.0	2.5	0.901	33.5	2.4	33.5	1.5	1.000
Pressure range of IVC-Occlusion	19.7	4.2	25.1	2.8	0.3	18.1	3.9	17.8	2.5	0.954
Steady state hemodynamics										
Heart rate (Hz)	75.6	4.2	72.4	4.1	0.609	88.9	7.6	73.4	3.3	0.105
End-systolic pressure (mmHg)	75.5	5.1	77.9	5.1	0.761	92.1	2.2	81.5	4.4	0.075
End-diastolic pressure (mmHg)	11.3	2.1	15.7	2.8	0.286	24.9	1.8	27.3	1.7	0.371
dP/dt max (mmHg/mL)	1071.4	70.7	1109.9	76.6	0.735	1582.0	56.6	1320.1	80.3	0.029*
dP/dt min (mmHg/mL)	− 1044.9	77.4	− 1015.2	71.7	0.789	− 1194.2	67.0	− 897.8	87.8	0.027*
End-systolic volume (mL)	34.3	3.4	65.8	7.7	0.006*	46.5	2.5	90.8	10.5	0.004*
End-diastolic volume (mL)	102.4	9.5	145.6	12.7	0.027*	154.3	5.8	210.8	11.0	0.001*
Stroke volume (mL)	68.1	7.2	79.8	7.4	0.303	107.8	6.3	120.0	9.1	0.326
Cardiac output (mL/min)	5150.6	586.7	5753.4	644.8	0.529	9620.0	1023.6	9290.3	898.4	0.813
Ejection fraction (%)	66.3	2.3	55.0	2.6	0.009*	69.6	1.9	57.1	3.6	0.017*
Stroke work (mJ)	649.2	84.3	3258.4	1049.3	0.032*	3032.4	1205.4	1960.5	876.5	0.474
Max. power (mW)	8569.2	909.9	8542.8	997.1	0.389	16,756.1	1135.1	10,012.5	1713.4	0.010*
Preload adjusted max. power (mW/mL^2)	0.879	0.123	0.440	0.050	0.011*	0.717	0.075	0.301	0.076	0.002*
Pressure volume area (mJ)	858.1	132.4	1091.4	141.5	0.268	1397.3	99.1	1433.8	145.9	0.851
Potential energy (mJ)	208.7	51.8	358.0	58.0	0.084	334.5	47.4	341.8	47.0	0.916
Efficiency (%)	77.0	2.2	68.9	2.9	0.053	76.5	2.8	65.4	9.8	0.307
Tau (Mirsky) (ms)	63.1	4.3	71.7	4.3	0.204	61.2	3.5	81.3	5.2	0.008*
ESPVR analysis										
E es (mmHg/mL)	3.28	0.21	2.09	0.16	0.000*	2.97	0.26	1.69	0.25	0.005*
ESPVR volume axis intercept (mL)	− 11.9	3.2	− 3.0	8.5	0.4	− 16.7	5.5	− 18.7	12.3	0.885
EDPVR analysis										
Stiffness constant ß	0.020	0.008	0.026	0.007	0.613	0.009	0.002	0.004	0.001	0.036*
Curve fitting constant a	4.94	1.63	6.59	2.28	0.566	8.93	2.15	13.03	1.85	0.178
Diastolic Capacitance at 20 mmHg	117.0	9.4	114.5	14.1	0.9	109.1	17.3	123.6	31.2	0.707
Preload recruitable stroke work										
Preload rectruitable stroke work (mmHg)	61.05	4.33	42.38	2.77	0.003*	67.88	4.70	49.63	4.38	0.016*
PRSW V0	5.2	5.8	4.9	12.2	1.0	31.2	6.0	27.2	12.7	0.791
dP/end-diastolic volume regression										
dP/EDV	3.63	1.09	1.94	1.02	0.303	6.29	1.22	1.52	0.27	0.002*
dP/EDV V0	− 383.1	136.9	281.5	366.4	0.1	− 134.4	94.9	− 1043.2	266.3	0.013*
Echo										
Stroke volume (echo-derived)	67.9	7.5	79.5	7.3	0.3	108.3	6.9	118.1	9.7	0.457
CMR parameters										
Heart rate (Hz)	72.2	2.3	71.6	4.6	0.9	71.1	5.9	64.6	5.6	0.454
Stroke volume (mL)	70.8	9.6	81.6	7.8	0.4	109.8	5.5	119.0	7.9	0.409
End-diastolic volume (mL)	103.0	13.3	148.3	12.7	0.0*	157.7	6.9	214.4	14.0	0.008*
End-systolic volume (mL)	31.7	4.0	66.7	7.6	0.0*	47.9	2.2	95.4	11.1	0.003*
Stroke volume (mL)	70.8	9.6	81.6	7.8	0.4	109.8	5.5	119.0	7.9	0.409
Ejection fraction (%)	68.8	2.2	55.1	2.7	0.0*	69.6	1.0	56.2	3.0	0.002*
Cardiac output (mL/min)	5.0	0.6	5.7	0.4	0.4	7.7	0.4	7.4	0.4	0.648

*$p < 0.05$

Asterisk (*) marks significant test results ($p < 0.05$). All significant effects are large (Cohen's $d > 0.8$)

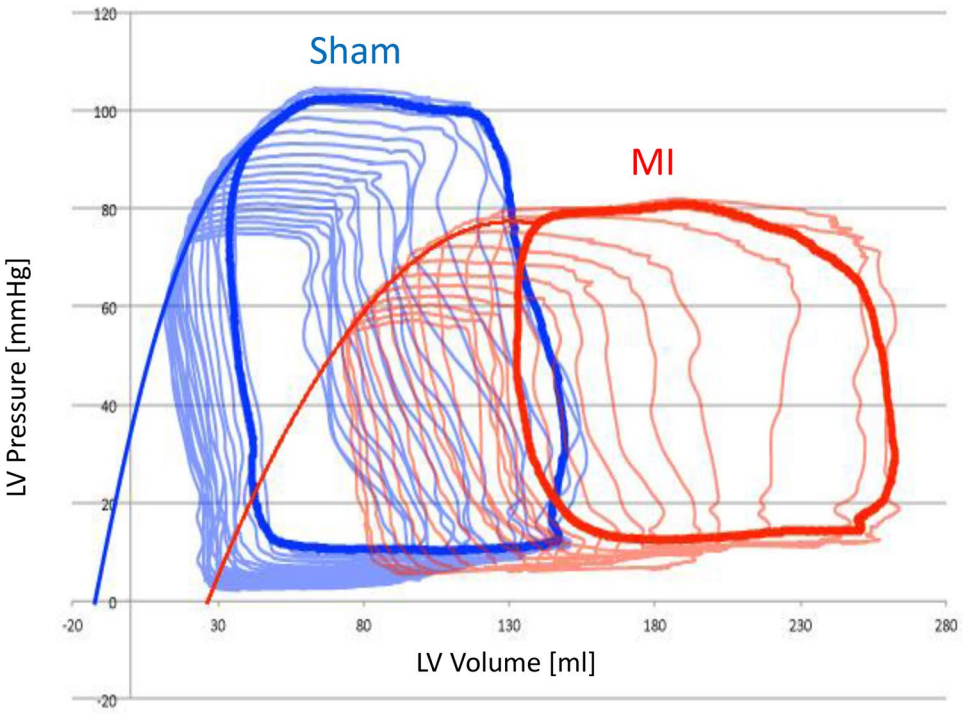

Fig. 3 Representative PV-loop recordings of an animal post-MI (red) and a sham animal (blue). Preload reduction was achieved by temporary balloon occlusion of the IVC and allows for calculation of preload independent parameters of systolic and diastolic LV function. Post-MI loop was taken at day 112 post myocardial infarction

Discussion

Despite conventional drug therapies as well as cardiac resynchronization- and defibrillator devices there is no cure for HF and the disease progresses relentlessly [1, 2]. Innovative therapies such as cardiac stem cell therapy or myocardial gene therapy offer the possibility to target the underlying causes of the disease and represent promising approaches to optimize clinical treatment of HF [3, 7, 16]. Reliable and thoroughly characterized large animal models of HF are a critical link in order to translate basic research concepts into clinical therapies [5]. Equally important, adequate techniques and valid analytic tools are necessary to analyze clinical parameters of cardiac function and LV structural remodeling in order to investigate the impact of novel therapeutic strategies.

Since the major proportion of HF etiology is ischemic cardiomyopathy we used a preclinical large animal model of pig post-MI HF being already extensively characterized by our group and others [1, 8, 9]. Most importantly, distinct myocardial gene therapy approaches were already successfully performed using this model [8, 9].

We show that the 72 h high sensitive troponine T (hsTnT) in peripheral blood correlates with myocardial infarct size quantified by cardiac MRI which is in line with previous studies in humans [12]. Therefore, the 72 h hsTnT might be used for group matching prior gene- or stem cell therapy and thus homogenize treatment groups.

Pigs presented significant structural remodelling of the LV and mild-to moderate HF due to mid-size myocardial infarction as determined by cardiac MRI 56 and 112 days post-MI. Moreover, LV ejection fraction and further distinct preload-independent functional properties of the LV such as PRSW and ESPVR were significantly reduced 56 and 112 days post-MI. In contrast, preload-dependent LV systolic parameters such as +dP/dt and parameters of diastolic function of the LV such as EDPVR, Tau (Mirsky) and stiffness constant β (dP/dV) were significantly deteriorated only at day 112, which might be caused by further deterioration of LV function occurring over time and being a characteristic of HF [1, 2]. Hence, assessment of LV function using preload-independent parameters acquired by admittance-derived PV loop analysis appears more sensitive as compared to solely pressure/time-based measurements such as ± dP/dt and might reduce the risk to miss significant hemodynamic effects. Analysis of hemodynamic effects of novel gene-based or stem-cell derived approaches should therefore include PV-loop measurements reducing the risk to overlook potential therapeutic effects.

We compared cardiac MRI as the gold standard to characterize structural myocardial remodeling and LV volumetry with admittance-derived PV-loop analysis using a pig post-MI HF model. LV volumetry and function as determined by distinct parameters such as ESV, EDV and EF revealed an excellent correlation between admittance-derived PV-loop analysis and cardiac MRI demonstrating that ESV and EDV

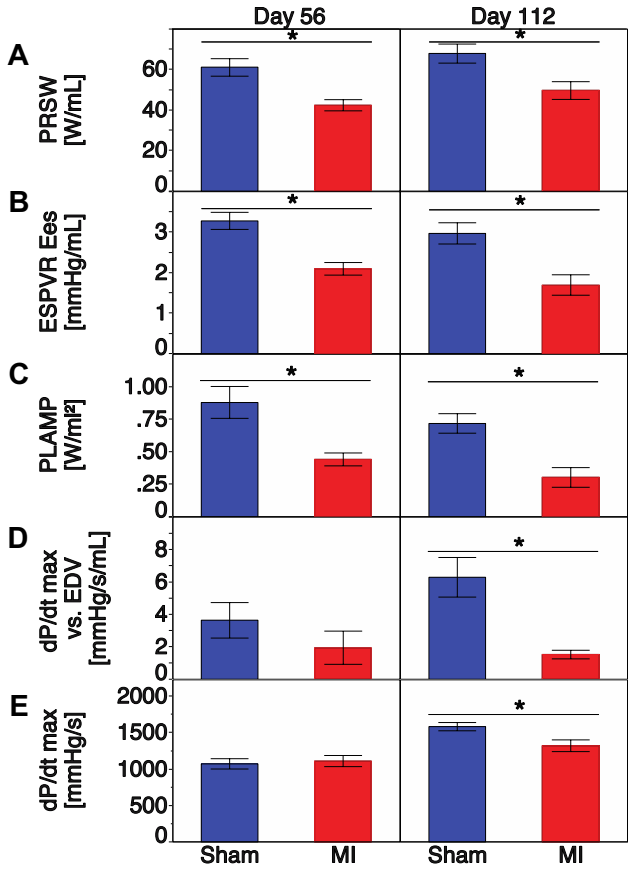

Fig. 4 PV-loop analysis of systolic left ventricular function 56 and 112 days post-MI and sham operation. Preload-dependent parameters: dP/dt max, dP/dt max versus EDV and preload adjusted maximum power (PLAMP). Preload-insensitive parameters: end-systolic pressure volume relationship (ESPVR Ees) and preload recruitable stroke work (PRSW). Mean ± SEM, *p < 0.05

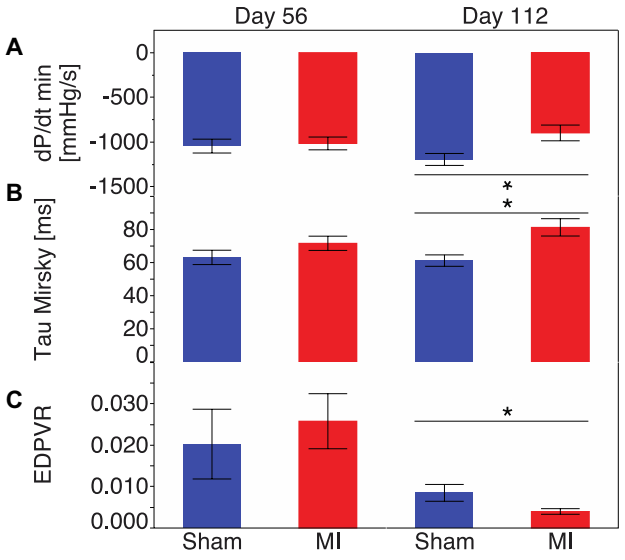

Fig. 5 PV-loop analysis of diastolic left ventricular function 56 and 112 days post-MI and sham operation. Preload-dependent parameters: dP/dt min and Tau Mirsky. Preload-insensitive parameter: end-diastolic pressure volume relationship (EDPVR). Mean ± SEM, *p < 0.05

as acquired by PV-loop are valid against established cardiac MRI. Our data is in line with Lin et al. using healthy animals [10]. In a more complex cardiac anatomy of a post-MI HF model, eccentrically shaped and with scar formation, our findings are in line with a study from van Hout and co-workers also using a pig post-MI HF model, which was induced by temporary occlusion of the left anterior descending (LAD) coronary artery [11]. Interestingly, von Hout et al. "failed to establish a significant correlation between either ESV or EF with the infarct size" using admittance-derived PV-loop analysis. In contrast, in our study, using a model of temporary LCX occlusion, a significant inverse correlation between admittance-derived EF and MRI derived infarct size could be found both at 56 and 112 days post-MI (Fig. 7). Mean infarct size was similar in both studies.

Overall, cardiac MRI and admittance-derived PV-loop analysis show an excellent correlation and thus admittance derived pressure volume loop analysis allows for precise assessment of systolic and diastolic left ventricular function. Cardiac MRI and PV-loop analysis complement each other since MRI offers the advantage to assess structural remodelling and regional myocardial function. Moreover, myocardial inflammation and scar formation can be identified and distinguished using cardiac MRI [17, 18]. PV-loop analysis allow for preload-independent measurements increasing the sensitivity to detect cardiac dysfunction or potential therapeutic effects, respectively [13, 14].

Temporary occlusion of the LCX using a preclinical pig large animal model causes global cardiac dysfunction and LV remodelling. Infarct size correlates with the hsTnT at 72 h facilitating the pre-therapeutic screening of post-MI animals and proper selection of HF animals. Cardiac MRI and PV-loop analysis complement each other in terms of characterizing LV remodelling and myocardial function. MRI and PV-loop analysis of ESV, EDV and EF show excellent correlation between both techniques.

Combination of cardiac MRI and PV-loop analysis should be used as the gold standard to comprehensively characterize LV dysfunction and LV remodelling in preclinical testing of stem-cell- or gene therapy in preclinical large animal models of HF.

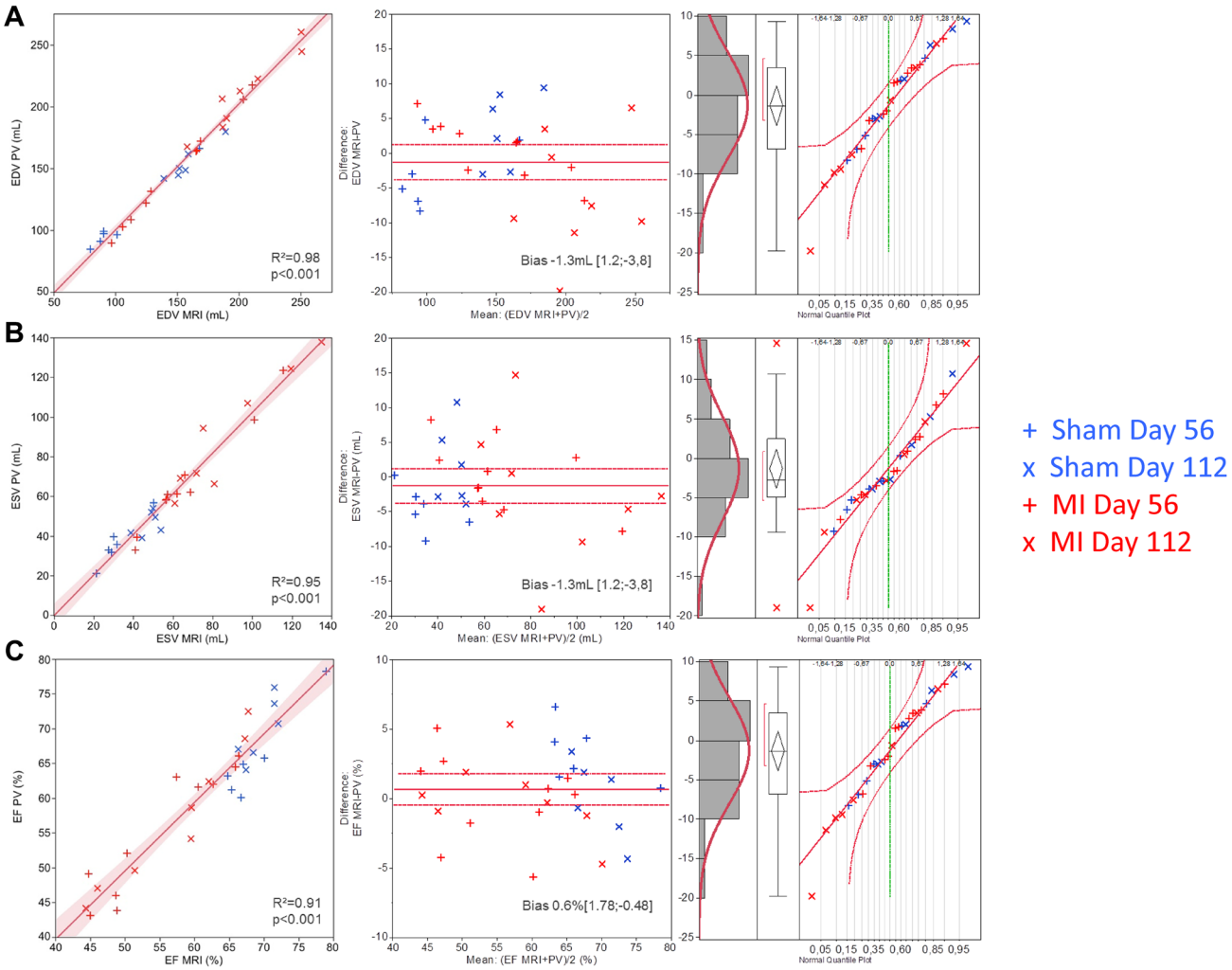

Fig. 6 Bland-Altman method comparison of admittance-derived PV-loop and cardiac MRI analysis of left ventricular myocardial function in post-MI and sham animals. **a** End-diastolic volume (EDV), **b** end-systolic volume (ESV), **c** ejection fraction (EF)

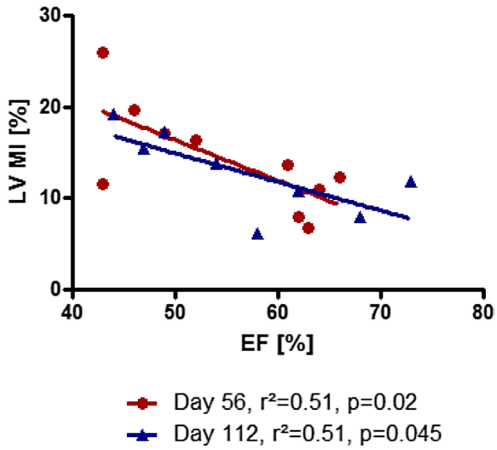

Fig. 7 Correlation of admittance-derided PV-loop ejection fraction (EF) and MRI derived infarct size. Analysis reveals significant inverse correlation between EF and infarct size at both 56 and 112 days. *LV MI (%)* LV area of cardiac MRI Gadolinium late enhancement, *EF* ejection fraction. Linear Regression

Funding This work was supported in part by grants from the Deutsche Forschungsgemeinschaft (RA 1668/3-1 to Philip W. Raake and PM 562/1-1 to Patrick Most) and the Bundesministerium für Bildung und Forschung (01GU0527 to Patrick Most and Hugo A. Katus). This study was further supported by grants of the National Institute of Health (RO1 HL92130 and RO1 HL92130-02 S1 to Patrick Most) and the DZHK ('Deutsches Zentrum für Herz-Kreislauf-Forschung'—German Centre for Cardiovascular Research).

Compliance with the ethical standards

Conflict of interest All authors declare that they have no conflict of interest.

References

1. Benjamin EJ, Virani SS, Callaway CW, Chamberlain AM, Chang AR, Cheng S, Chiuve SE, Cushman M, Delling FN, Deo R, de Ferranti SD, Ferguson JF, Fornage M, Gillespie C, Isasi CR, Jiménez MC, Jordan LC, Judd SE, Lackland D, Lichtman JH,

Lisabeth L, Liu S, Longenecker CT, Lutsey PL, Mackey JS, Matchar DB, Matsushita K, Mussolino ME, Nasir K, O'Flaherty M, Palaniappan LP, Pandey A, Pandey DK, Reeves MJ, Ritchey MD, Rodriguez CJ, Roth GA, Rosamond WD, Sampson UKA, Satou GM, Shah SH, Spartano NL, Tirschwell DL, Tsao CW, Voeks JH, Willey JZ, Wilkins JT, Wu JH, Alger HM, Wong SS, Muntner P (2018) Heart Disease and Stroke Statistics - 2018 Update: a Report from the American Heart Association. Circulation 137(12):e67–e492

2. McMurray JJ (2010) Clinical practice. Systolic heart failure. N Engl J Med 362:228–238
3. Anversa P, Kajstura J, Rota M, Leri A (2013) Regenerating new heart with stem cells. J Clin Invest 123(1):62–70
4. Byrne MJ, Power JM, Preovolos A, Mariani JA, Hajjar RJ, Kaye DM (2008) Recirculating cardiac delivery of AAV2/1SERCA2a improves myocardial function in an experimental model of heart failure in large animals. Gene Ther 15(23):1550–1557
5. Dixon JA, Spinale FG (2009) Large animal models of heart failure: a critical link in the translation of basic science to clinical practice. Circ Heart Fail 2:262–271
6. Lai NC, Roth DM, Gao MH, Tang T, Dalton N, Lai YY, Spellman M, Clopton P, Hammond HK (2004) Intracoronary adenovirus encoding adenylyl cyclase VI increases left ventricular function in heart failure. Circulation 110(3):330–336
7. Pleger ST, Boucher M, Most P, Koch WJ (2007) Targeting myocardial beta-adrenergic receptor signaling and calcium cycling for heart failure gene therapy. J Card Fail 13(5):401–414
8. Pleger ST, Shan C, Ksienzyk J, Bekeredjian R, Boekstegers P, Hinkel R, Schinkel S, Leuchs B, Ludwig J, Qiu G, Weber C, Raake P, Koch WJ, Katus HA, Müller OJ, Most P (2011) Cardiac AAV9-S100A1 gene therapy rescues post-ischemic heart failure in a preclinical large animal model. Sci Transl Med 3(92):92ra64
9. Raake PW, Schlegel P, Ksienzyk J, Reinkober J, Barthelmes J, Schinkel S, Pleger S, Mier W, Haberkorn U, Koch WJ, Katus HA, Most P, Müller OJ (2013) AAV6.βARKct cardiac gene therapy ameliorates cardiac function and normalizes the catecholaminergic axis in a clinically relevant large animal heart failure model. Eur Heart J 34(19):1437–1447
10. Lin HY, Freed D, Lee TW, Arora RC, Ali A, Almoustadi W, Xiang B, Wang F, Large S, King SB, Tomanek B, Tian G (2011) Quantitative assessment of cardiac output and left ventricular function by noninvasive phase-contrast and cine MRI: validation study with invasive pressure-volume loop analysis in a swine model. J Magn Reson Imaging 34(1):203–210
11. Van Hout GP, Jansen of Lorkeers SJ, Gho JM, Doevendans PA, van Solinge WW, Pasterkamp G, Chamuleau SA, Hoefer IE (2014) Admittance-based pressure-volume loops versus gold standard cardiac magnetic resonance imaging in a porcine model of myocardial infarction. Physiol Rep 2(4):e00287
12. Licka M, Zimmermann R, Zehelein J, Dengler TJ, Katus HA, Kübler W (2002) Troponin T concentrations 72 hours after myocardial infarction as a serological estimate of infarct size. Heart 87(6):520–524
13. Cingolani OH, Kass DA (2011) Pressure-volume relation analysis of mouse ventricular function. Am J Physiol Heart Circ Physiol 301(6):H2198–H2206
14. Burkhoff D, Mirsky I, Suga H (2005) Assessment of systolic and diastolic ventricular properties via pressure-volume analysis: a guide for clinical, translational, and basic researchers. Am J Physiol Heart Circ Physiol 289(2):H501–H512
15. Bland JM, Altman DG (1986) Statistical methods for assessing agreement between two methods of clinical measurement. Lancet 1(8476):307–310
16. Tilemann L, Ishikawa K, Weber T, Hajjar RJ (2012) Gene therapy for heart failure. Circ Res 10(5):777–793
17. Steen H, Nasir K, Flynn E, El-Shehaby I, Lai S, Katus HA, Bluemcke D, Lima JA (2007) Is magnetic resonance imaging the 'reference standard' for cardiac functional assessment? Factors influencing measurement of left ventricular mass and volumes. Clin Res Cardiol 96(10):743–751
18. Yilmaz A, Ferreira V, Klingel K, Kandolf R, Neubauer S, Sechtem U (2013) Role of cardiovascular magnetic resonance imaging (CMR) in the diagnosis of acute and chronic myocarditis. Heart Fail Rev 18(6):747–760